AN OPTIMIZED APPROACH OF DEEP NEURAL NETWORK FOR LUNG CANCER IMAGE ANALYSIS

Dr. N. Rajalakshmi[1*], Dr. K. Narayanan[2], Swathy K[1], Dr. P. Manimegalai[3], Elangkathir G[1], Irfana B[1], Priyadharshini P[1], Santhosh P[1]

[1*]Department of Biomedical Engineering, Dhanalakshmi Srinivasan College of Engineering, Coimbatore, Tamil Nadu, India

[2]Department of Computer Science Engineering, Thanthai Periyar Government Institute of Technology, Vellore, Tamil Nadu, India

[3]Department of Biomedical Engineering, Karunya Institute of Technology and Sciences, Coimbatore, Tamil Nadu, India

[1]Professor (Dr. N. Rajalakshmi) | Email: praniraji1@gmail.com

[2]Assistant Professor (Dr. K. Narayanan) | Email: krishnasamynarayanan@gmail.com

[1]Assistant Professor (Swathy K) | Email: Swathyraji2226@gmail.com

[3]Associate Professor (Dr. P. Manimegalai) | Email: manimegalai.vairavan@gmail.com

[1]UG Scholar (Elangkathir G) | Email: gelangkathirelangkathir@gmail.com

[1]UG Scholar (Irfana B) | Email: Irfanaisak768@gmail.com

[1]UG Scholar (Priyadharshini P) | Email: priyadharshini0661@gmail.com

[1]UG Scholar (Santhosh P) | Email: santhoshs6924@gmail.com

***Corresponding Author:** Dr. N. Rajalakshmi, Professor, Department of Biomedical Engineering, Dhanalakshmi Srinivasan College of Engineering, Coimbatore, Tamil Nadu, India | Email: praniraji1@gmail.com

Abstract—To facilitate early lung cancer diagnosis, this paper introduces a hybrid feature concatenation framework that merges semantic and texture information from lung CT images. Semantic features are derived using a pretrained ResNet50 model, while texture features are extracted through handcrafted statistical descriptors based on histogram properties. This integration produces a high-dimensional feature vector, which is subsequently reduced using Principal Component Analysis (PCA) to address dimensionality issues. The refined feature set is classified into benign and malignant categories using a Support Vector Machine (SVM). The analysis using SHAP plots shows that features contributing to malignant predictions are typically positive, whereas features associated with benign predictions are negative. Performance evaluation on 826 CT image slices yielded an accuracy and F1-score exceeding 95%, thereby validating the effectiveness of the proposed method for lung cancer classification.

***Keywords*-**Lung cancer, deep learning, radiometric,semantic, hybrid feature, explainablility;

How to cite this article: Rajalakshmi N, Narayanan K, Swathy K, Manimegalai P, Elangkathir G, Irfana B, Priyadharshini P, Santhosh P. An optimized approach of deep neural network for lung cancer image analysis. Int J Drug Deliv Technol. 2026;16(73s): 80-90. DOI: 10.25258/ijddt.16.73s.10

I. INTRODUCTION

Lung cancer is the predominant cause of mortality among cancer-related deaths. 80% of lung cancers are caused due to smoking tobacco. It is expected that more than 28 million cases will be affected by cancer in 2040, which is a 47% increase from the 2020 estimation. The most cost-effective primary prevention of this deadly disease is encouraging social education regarding the consequences of smoking and helping smokers to quit smoking. Because lung cancer leads to other diseases like stroke, asthma, chronic obstructive pulmonary disease, and cardiovascular diseases. Secondary prevention involves the diagnosis of cancer at an earlier stage and treatment by surgery or stereotactic body radiation therapy (SBRT)[2].

The computerized analysis of 3D scans in computed tomography (CT) and positron emission tomography (PET) has shown improved diagnosis and higher accuracy in lesion prediction, which has assisted in clinical practice. Low-dose computed tomography (LDCT)-based screening is a promising tool for predicting malignancies in pulmonary

nodules. However, differentiating between benign and malignant nodules remains a clinical challenge. Radiomics has emerged as a transformative approach in which PET/CT scans or medical images are converted into quantitative image data to extract high-dimensional features. When utilizing a radiomics pipeline for preprocessing, segmentation by calculating the region of interest (ROI) and feature extraction from LDCT images, it improves the malignant nodule classification, and structured radiomic biomarkers enhance the prognostic model [3] [4] [5].

Non-small cell lung cancer (NSCLC) is a major type of lung cancer with adenocarcinoma (ADC), squamous cell carcinoma (SCC), large cell carcinoma (LCC), and no other specified (NOS) as histological types. The radiomics feature extraction has quantitative metrics, which include 1) shape feature, 2) first and higher order statistical feature, and 3) texture features such as gray-level co-occurrence matrix (GLCM), gray-level run length matrix (GLRLM), gray-level size zone matrix (GLSZM), neighborhood gray-tone difference matrix (NGTDM), and gray-level dependence matrix (GLDM) [6].

In recent years, machine learning (ML) algorithms, such as XGBoost, support vector machine (SVM), random forest (RF), logistic regression, and LightGBM, have been integrated with radiomics to develop a non-invasive predictive model for high performance [7]. Radiomic features, along with deep learning (DL) approaches, particularly convolutional neural networks (CNN), have automated the process of feature extraction from CT data and identified the histological phenotypes of NSCLC [8].

Artificial intelligence (AI) plays a major role in screening, diagnosing, predicting treatment approaches, and suggesting precision medicine. AI with computer-aided detection (CAD) helps in distinguishing malignant and benign nodules automatically with higher sensitivity and optimal imaging quality [9] [10]. Despite their high capability in predicting malignancy, ML and DL models with AI operate as opaque ‘black - box’ systems that limit clinical adoption, ethical implementation, and regulatory approval [11].The integration of DL-CNN with AI develops a transparent and interpretable model for safe decision-making support by applying explainable AI (XAI) techniques. The explainable layer consists of Shapley additive explanations (SHAP) to visualize positive and negative evidence of the model, which grades the cancer as normal, benign, and malignant. XAI feature is still enhanced by local interpretable model agnostic explanations (LIME) and gradient-weighted class activation mapping (Grad-CAM), which highlights the critical regions of images and provides visual explanations for the clinical outputs [12] [13] [14].There are several lung cancer imaging datasets available publicly. They are the Iraq-oncology teaching hospital of the national center for cancer diseases (IQ-OTH/NCCD), Lung image database consortium (LIDC), Image database resource initiative (IDRI), The cancer imaging archive (TCIA), NSCLC radio genomics, National lung screening trial (NLST), etc., which are used for lung cancer analysis to train and test the model for robust performance[15].

The research gaps identified are multi-modal data integration, automated segmentation, image enhancement, feature extraction, generalization, and data analysis, which are to be focused in the upcoming research. So that the malignant lung nodule is identified at an early stage and the patient’s outcomes are improved. This improves the diagnosing tool with high accuracy, making wise decisions to support clinicians in suggesting precision treatment and medicine [16].

In this proposed work, we have presented a framework incorporating radiomics for feature extraction from medical images and a CNN for the classification of lung nodules with XAI for an accurate, transparent, and interpretable lung malignancy prediction model. Various performance metrics are used to assess the efficacy of this model.

This paper summarized as follows. Section I provides a brief introduction to lung cancer and its predictive methodologies. Section II describes the literature survey of conventionalmodels and techniques with the research gap. Section III explains the proposed methodologies and calculations of performance metrics. Section IV demonstrates the results of the proposed model, and Section V concludes the study with future work.

II. Related works

Haque et al. (2025) introduced a concatenation of two different CNNs with a multi-layer perceptron and multi-head attention mechanism for the classification of lung cancer automatically by achieving a high accuracy of 99.54%, 99.97% AUC, 99.31% of precision using IQ-OTH/NCCD datasets. This model was harnessed with an AI technique of Grad-CAM and SHAP for highlighting critical regions of the images, allowing real-time visualization using the Gradio user interface, which offered a user-friendly tool for the diagnosis. Despite these efficiencies, the real-world clinical setting was not validated on diverse datasets, and the minor fluctuations in the highlighted regions need to be concentrated in future efforts.

Marjolein et al. (2021) proposed a lung cancer prediction of CNN (LCP-CNN) to predict the malignant lung nodule. This model was trained on the US NLST dataset and validated on CT scans to identify benign nodules with a high sensitivity of 99%, an AUC of 94.5%, and a high accuracy in ruling out malignancy of 22% in about one-fifth of the patients from small to intermediate-sized nodules. Though the possibility of predicting malignancy in larger lung nodules of size 30 mm is less, and limits clinical

applicability, this tool, with high sensitivity, identified benign nodules incidentally by avoiding follow-up procedures for 18.5% of patients.

Jiaying et al. (2024) developed a radiomics model for the classification of benign and malignant lung nodules. To overcome high false positive rates of LDCT images, synthetic LDCT images are used that are generated from standard-DCT (SDCT**)** scans in the LIDC-IDRI dataset that are degraded in the sinogram domain. A systematic pipeline including SHAP analysis optimized the radiomics feature sets, and multiple ML models were evaluated, trained on degraded SDCT, and tested on LDCT to achieve an accuracy of 0.81, an AUC-ROC score of 0.87, sensitivity and specificities of 0.76 and 0.85, respectively. However, this study focused mainly on developing segmentation methods rather than detecting and classifying lung nodules, with limited validation on external datasets using DL models for improved clinical usability.

Aonpong et al. (2021) presented two models of genotype-guided radiomics (GGR) method to predict the recurrence of NSCLC at a low cost. The first gene estimation model estimated the gene expressions from the features of radiomics and extracted deep features from CT scans in radiogenomics datasets. Then this estimated genotype information predicted the early recurrence in the second training model. This GGR model achieved the prediction accuracy of 83.28% and AUC of 0.7667 over ResNet50 and the existing radiomics method, which can still be improved by increasing the training datasets.

Lin et al. (2024) demonstrated a CT-based radiomics for the classification of histological typing and clinical stage of patients with NSCLC. This study used 537 CT series from the TCIA database and extracted 107 quantitative radiomic features to feed as an input to ML classifiers. The random forest model has better performance for both histological typing and staging, with an AUC of 0.700 and 0.881, respectively. Among seven key features, the first order and texture radiomics features incorporated in the classification model provide a better non-invasive diagnostic tool for NSCLC. A smaller dataset, lack of external validation on different images, and imbalanced sample size are some of the limitations of this model.

Zahra et al. (2021) employed a high-dimensional radiomics pipeline for the classification of SCC, ADC, LCC, and NOS in NSCLC patients from CT images. Wrapper algorithm and multivariate adaptive regression splines were used to extract 1443 radiomics features, and multinomial logistic regression with 1000 bootstrapping samples was employed to classify the four subtypes of NSCLC. The gray-level size zone matrix (GLSZM) highlighted the most discriminative features and achieved an accuracy of 0.865, which made it a more non-invasive approach in prediction and treatment. The main limitation of this model is its single-center retrospective design, single modality dataset without external validation, which restricted the generalizability.

Hung et al. (2023) integrated an interpretable AI model with a 3D hierarchical semantic CNN (HSNet) for the automatic diagnosis of lung cancer in the LIDC-IDRI CT lung nodule images with different semantic attributes and four-fold cross-validation. HSNet used optimization strategies such as cyclic learning rate, early stopping strategy, random weight averaging, and adjustment of model parameters, which refined the accuracy from 93.22% to 97.84% that differentiated benign and malignant nodules. This generates automatic, explainable diagnostic reports to assist doctors during examinations. This research lacks multimodal DL models and a larger amount of dataset evaluation, which limits real-world generalizability.

Hossain et al. (2025) innovated a hybrid CNN and singular value decomposition (CNN-SVM) ensemble method for multiclass and binary lung cancer detection by achieving an accuracy of 99.49% and 100%, respectively, from the Kaggle chest CT images. CLAHE is employed to enhance the contrast of the images, and Grad-CAM, as an explainable AI (XAI) technique highlighted the key distinct features in the regions of the CT scan. CNN-SVM reduced the dimensionality, and the extracted features are processed by the ML algorithms with a voting ensemble approach, which improved its robustness, transparency, and reliability. However, lack of using a transfer learning approach on multi-center datasets, advanced preprocessing techniques, restricts the clinical applicability in early lung cancer detection.

Kesiku et al. (2025) presented a hybrid CNN-BiLSTM (Bidirectional long short-term memory networks) DL model, which is trained on MIMIC-IV clinical notes datasets for lung cancer detection. This study was evaluated on the Yelp review polarity dataset in which CNN extracted the local text patterns and BiLSTM long-range contextual in both directions to achieve an accuracy of 98.1% and MCC of 96.2%, which surpassed the performance of LSTM and BioBERT baselines. The SHAP values approach employed in this model provided valuable insights from the medical notes that influenced the better classification and detection of cancer nodules, making it a diagnostic tool for clinical decision support. This study can still be improved in model interpretability and training on diverse datasets with XAI.

Shimada et al. (2023) investigated an AI model with CT radiomics values in clinical stage 0-IA NSCLC patients for predicting pathological lymph node metastasis (pN). To detect the factors related to pN, 39 imaging factors from AI were extracted, and identified that IA3, solid part size, and average solid-CT values were associated with pN. In the

entire cohort, AUC and optimal cut-off values were 0.761 and 103 Hounsfield units, providing a sensitivity of 69%, 65% of specificity, and negative predictive values of 94%, which guided personalized need for surgery and postoperative treatments. The main limitation of this study is the use of preoperative CT images. Because of its low fidelity, some of the images were not processed successfully and lacked external validation.

Hunter et al. (2023) developed a model for early diagnosis of lung cancer in small lung nodules (≤15 mm) with improved stratification by validating larger datasets with external testing. Segmentation of multi-region CT images and LASSO regression extracted the 5 featured small nodule radiomics predictive vector (SN-RPV), which can split intermediate to risk group of patients using K-means clustering. The AUC of identifying malignant nodules by SN-RPV and radiologists were 0.78 and 0.75, respectively. The accuracy of the test set was 73%, which resulted in avoiding delayed or missed cancer diagnosis by radiologists. However, the model requires manual preprocessing and segmentation steps of images, which need to be automated for clinical implementation. Stratification requires a separate model, as subsolid nodules and ground glass nodules were excluded in this model.

Hunter et al. (2022) proposed a DL based nnUNet model incorporated with radiomics features for the automatic segmentation and classification of large lung nodules (≥ 15 mm) by validating 838 CT scans. The performance of the large nodule radiomics predictive vector (LN-RPV) was compared with the radiologist's Brock and Herder scores. AUC of LN-RPV and radiologists were analyzed to be 0.83 and 0.75, for baseline solid nodules. AUC of LN-RPV was 0.87, Brock score was 0.67, and Herder score was 0.83, which showed that LN-RPV had higher performance in classifying and segmenting large lung nodules accurately, which reduced the risk of delayed treatment. The external validation with a larger dataset is required for generalization; multivariate analysis into a single program needs to be focused, along with DeLong's test, for an interpretable clinical model.

Hamaad et al. (2025) integrated a custom CNN and XAI with Grad-CAM to classify lung cancer from the datasets of CT images and achieved an accuracy of 93.06%. The interpretable features with Grad-CAM visualization made the model more reliable and transparent in earlier diagnosing malignancy subtypes with explainable clinical reports. The data augmentation and regularization techniques incorporated in diverse datasets resulted in robust performance with generalization. Despite the significance, this study on Grad-CAM highlighted only the area of interest in CT and did not provide the decision support process. The computational demand is higher, which restricts the usability of real-time applications and misclassifies malignancies with subtle differences.

Chen et al. (2025) studied a model incorporating CNN with CT radiomics to diagnose the lung ground glass nodule (GGN) and provide personalized treatment support. MATLAB's DL tool is used to train the CNN model, Gaussian filtering for CT image preprocessing, and segment manually to identify the region of interest (ROI). The accuracy, AUC, sensitivity, and specificity of this model was 85.07%, 0.887, 82.4%, and 75.5%, respectively, which surpassed the existing model's performance. Maximum diameter, mean, volume, and consolidation–to-tumor ratio (CTR) gives the infiltrative nature of the malignancies. However, the limitations include single center retrospective design, labor intensive study, and limited predictive performance restricted to clinical practice.

Ma et al. (2024) employed the fusion graph convolution network (FGCN) for the survival prediction of NSCLC in multimodal graph data. The strategy of Top K Pooling strategy was introduced to reduce redundancy, excessive noise, model complexity, and improve feature map processing. The SAGE graph convolution layer improves the convergence and achieved C-index value of 0.76, which is higher than the existing model. This model uses only two types of clinical and image data, which does not fully explore the intrinsic interaction during feature extraction, and requires a larger dataset to improve model performance. If the density of features for each patient is different, then the Top K Pooling strategy is not suitable. These are all some shortcomings to overcome.

The above studied literature showed better results in predicting lung malignancies and achieved higher performance in classifying the histological phenotypes. Despite the advantages, some limitations need to be concentrated. The proposed work develops a robust, interpretable, and generalizable framework incorporating CNN and radiomics features with XAI techniques, which enhance the clinical applicability of lung cancer prediction.

III. PROPOSED METHOD

To enable early diagnosis of lung cancer, this paper proposes a hybrid feature concatenation framework that integrates semantic and texture information from lung CT images. Semantic features are extracted using a pretrained ResNet50 model, while texture features are obtained through handcrafted statistical descriptors derived from first order and second-order histogram properties of image. The fusion of these heterogeneous features results in a high-dimensional feature vector. To address the resulting dimensionality and redundancy, Principal Component Analysis (PCA) is employed for feature reduction. The reduced feature set is then classified into benign and

malignant categories using a Support Vector Machine (SVM). Flow diagram of proposed system is given in Fig1.

A. Image Dataset

The SPIE-AAPM Lung CT Challenge dataset, which consists of thoracic CT scans annotated by radiologists, is used to analyse the performance of the proposed method in identifying lung nodules as benign or malignant. These two classes were labelled as class 0 for benign and class 1 for malignant.

For analysis, a total of 4,130 CT slices were selected from the dataset. Among these, 3,304 slices were used for training, and the remaining 826 slices were used for testing. The dataset exhibits large variability in lesion size, shape, contrast, and texture, which makes the classification problem clinically realistic and challenging.

B. Pre-Processing Stage

To ease the semantic feature extraction process, the images were resized to [224 224 3] and its pixel values were normalized using Z score normalization as follows;

$$I_n = \frac{(I - \mu)}{\sigma} \tag{1}$$

Equation 1 is used to obtain the normalized image I_n by using the mean and standard deviation of the pixels in input CT slices I. These normalized images are then subjected to feature extraction to highlight the semantic and texture information for identifying the benign and malignant cancer CT slices

C. Feature Extraction

The normalized images were subjected to feature extraction using deep learning and statistical analysis to highlight the difference between malignant and benign CT slices. The techniques used in this hybrid feature extraction process is explained below.

1) Semantic feature extraction

A pretrained CNN called RESNET 50 is used for extracting high level semantic features from the image and is presented as.

$$F_d = \Psi(I_n; \theta) \tag{2}$$

Using learnable parameters θ of CNN, the deep features F_d were extracted from the normalized image slices. These features highlight the tissue boundaries and intra nodular heterogeneity.

2) Statistical Radiomic Feature Extraction

The texture of information about tissues in the lung CT slice was also captured in a parallel manner using handcrafted radiometric features. These radiometric features were computed from the pixel intensity distribution, commonly referred to as the histogram. The intensity variations in the image are highlighted using first-order histogram properties, namely the mean and standard deviation. The corresponding formulas for calculating these first-order histogram properties are given as follows:

$$\mu = \frac{1}{MN}\sum_{x=1}^{M}\sum_{y=1}^{N} I_n(x,y) \tag{3}$$

The term μdenotes the average gray-level intensity of the normalized lung images. The terms $M$and Nrepresent the image dimensions, which are 224×224in this study. Similarly, the standard deviation is calculated as follows:

$$\sigma = \sqrt{\frac{1}{MN}\sum_{x=1}^{M}\sum_{y=1}^{N}(I_n(x,y) - \mu)^2} \tag{4}$$

The standard deviation σ helps to quantify the deviation of the pixel intensity distribution around the mean value of the image. Both first-order histogram properties describe the pixel intensity distribution in the image, whereas second-order histogram properties characterize the tissue structures and boundaries in lung CT images. The second order histogram properties are calculated using the grey level cooccurrence matrix (G). With the help of G, the following parameters namely contrast, homogeneity and energy are calculated as follows:

$$contrast = \sum_{i=0}^{G-1}\sum_{j=0}^{G-1}(i-j)^2 P(i,j) \tag{5}$$

$$homogeneity = \sum_{i=0}^{G-1}\sum_{j=0}^{G-1}\frac{(i,j)}{1+|i-j|} \tag{6}$$

$$Energy = \sum_{i=0}^{G-1}\sum_{j=0}^{G-1} P(i,j)^2 \tag{7}$$

Each GLCM property highlights different tissue texture characteristics. For example, contrast emphasizes the intensity variation and roughness of the texture, while homogeneity and energy describe the intensity distribution along the diagonal elements of the GLCM and the uniformity of pixel intensities. In overall, the statistical feature is calculated as follows:

$$F_S = [\,\mu, \sigma, contrast, homogeniety, energy] \tag{8}$$

Both this semantic feature from deep learning and radiomic feature from statistical analysis were combined as follows:

$$F = [F_d; F_S] \tag{9}$$

This hybrid feature of concatenation highlights the differences between benign and malignant lung cancer images by combining semantic and texture properties.

D. Hybrid feature fusion and PCA based feature reduction

The semantic features extracted from the deep learning architecture are high dimensional, which increases the overall feature vector size to 2053. This dimensionality is reduced to minimize computational complexity, such as training time and memory requirements, using a feature reduction technique known as Principal Component Analysis (PCA).

$$Z = xV_k \tag{10}$$

The term V_k denotes the top 30 eigenvectors selected from the PCA. These thirty vectors are highly influential for lung cancer classification, and their effectiveness is demonstrated through Grad-CAM and SHAP analyses in the following sections.

E. SVM based classification

The thirty vectors obtained from PCA are used for classification using an SVM classifier with an RBF kernel, as described below:

$$f(x) = w^T Z + b \tag{11}$$

The weights $w$and bias $b$in the classifier help to separate benign and malignant samples in the reduced feature space.

F. Explainability

To evaluate the feature reduction, the Grad-CAM and SHAP feature analysis were carried out. GRAD CAM highlights semantic features from deep learning contributing to predictions, while SHAP explains PCA feature contributions:

$$f(x) = \emptyset_0 \sum_{m=1}^{30} \emptyset_i \tag{12}$$

The term $\emptyset_0 \& \emptyset_i$ is the SHAP value of the initial feature and the i[th] PCA feature vector respectively.

G. Performance Metrics

The proposed method performance was evaluated using binary classification metrics like Accuracy, Precision, Recall, F1 score,and Specificity.

$$Accuracy = \frac{TN+TP}{TN+TP+FN+F} \tag{13}$$

$$Recall = \frac{TP}{TP+FN} \tag{14}$$

$$Specificity = \frac{TN}{TN+FP} \tag{15}$$

$$precision = \frac{TP}{TP+FP} \tag{16}$$

$$F1\ score = 2.\ \frac{Precision\ .Recall}{Precision + recall} \tag{17}$$

The terms TP and TN indicate the correct identification of benign and malignant cases, respectively, while FP and FN denote the misclassification of benign as malignant and malignant as benign. Using these metrics, the performance of the proposed method was evaluated, and the corresponding results are presented below section.

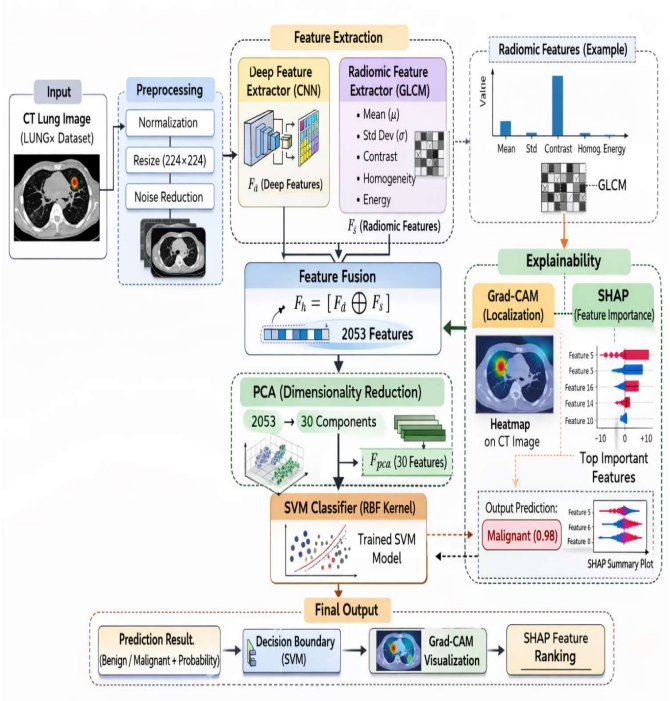

Figure1. Flow diagram of proposed approach

IV. RESULTS AND DISCUSSION

The proposed hybrid feature concatenation–based lung cancer classification model was implemented in Python using Google Co lab. The DICOM CT images were converted into JPG format and then subjected to a preprocessing step. The corresponding outputs for benign and malignant images are presented below.

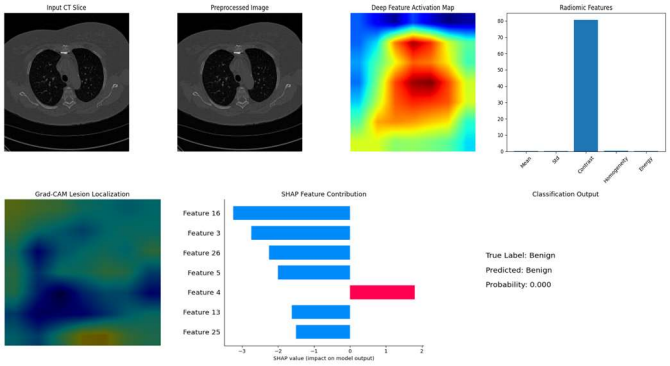

Figure 2. Benign output images

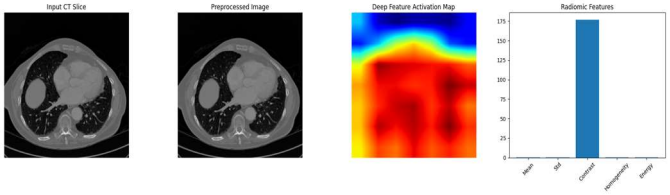

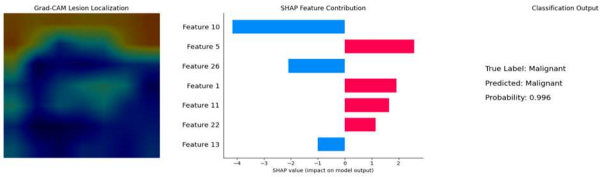

Figure 3. Malignant output image

The first two images in the top portions of Figures 2 and 3 represent the input and pre-processed benign and malignant CT image slices. The next two images illustrate the extracted deep and radiometric features of the input images.

The radiometric bar plot presents the radiometric feature values of the images. By comparing these values, it can be observed that the contrast value is higher for malignant images than for benign images, indicating that contrast is an important feature for image classification. Similarly, the activation map obtained from the deep learning model highlights the lesion regions that are useful for distinguishing between benign and malignant images.

The contribution of the proposed features is verified both statistically and visually using Grad-CAM and SHAP analyses, as shown in the bottom portions of Figures 2 and 3.

1) SHAP Analysis

In the SHAP plots, features that contribute toward malignant prediction are represented by positive values, whereas features contributing toward benign prediction are represented by negative values. As observed in the figures, most features for the benign class lie in the negative direction, while those for the malignant class lie predominantly in the positive direction.

2) Grad-CAM Findings

The hotter regions, such as red and yellow, highlight the lesion areas that are useful for identifying malignant nodules. In contrast, the cooler regions, such as blue and their combinations, indicate less significant contributions to the classification. It can also be visually verified from the Grad-CAM plots that no prominent regions are highlighted for benign identification.

3) Performance Analysis

The proposed method performance was evaluated on 826 CT image slices which comprises both malignant and benign images and its corresponding binary classification confusion matrix is presented in figure 4.

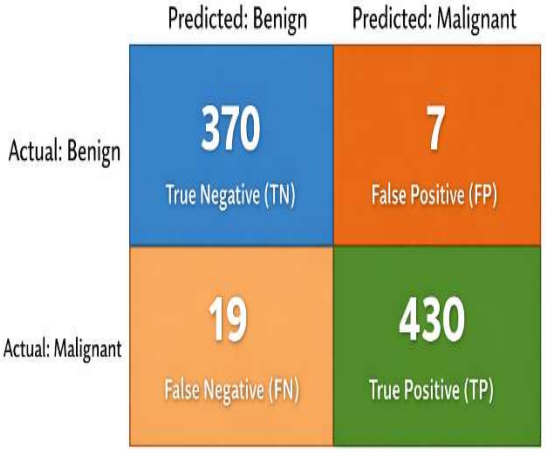

Figure 4. Confusion matrix

Based on figure 4, the classification of metrics for each image class and overall performance of the proposed method are presented in table 1 to 3 below.

Table 1. Malignant classification performance

Metric	**Li et al., (2024) (%)**	**Proposed Method (%)**
Precision (Malignant)	87.65	**98.4**
Recall / Sensitivity (Malignant)	88.57	**95.77**
F1-score (Malignant)	88.1	**97.06**

Table 2. Benign classification performance

Metric	Li et al., (2024) (%)	Proposed Method (%)
Precision (Malignant)	87.65	**98.4**
Recall / Sensitivity (Malignant)	88.57	**95.77**
F1-score (Malignant)	88.1	**97.06**

Table 3. overall classification performance

Metric	Li et al., (2024) (%)	Proposed Method (%)
Accuracy	88.04	**97.25**
Precision	87.65	**98.4**
Recall (Sensitivity)	88.57	**95.76**
F1-score	88.1	**97.06**
Specificity	87.5	**98.14**

From tables 1 to 3, the proposed method achieved higher accuracy and F1 score of above 95% in both individual and combined classes. The proposed method performance outperforms the existing work namely Tauguchi conventional fuzzy classifier by Li et al. (2024). The superior performance achieved with the hybrid feature concatenations. This makes the proposed framework suitable for clinical decision support. The explainability provided by Grad-CAM and SHAP improves proposed method's trustworthiness and transparency of automated predictions.

V. CONCLUSION AND FUTURE SCOPE

This study presented a hybrid deep–radiomic SVM-based framework for lung nodule classification using CT images from the LUNGx dataset. By integrating CNN-derived deep features with handcrafted radiomic descriptors, the model achieved improved robustness and discriminative performance. The proposed approach obtained 97% classification accuracy with strong precision and recall for malignant detection. Furthermore, the incorporation of Grad-CAM and SHAP enabled both spatial and feature-level interpretability, enhancing clinical trust in automated diagnosis. Future work will extend the framework to three-dimensional volumetric CT analysis and multi-class severity grading.

REFERENCES

[1] Lin, C. J., Lin, X. Q., & Jhang, J. Y. (2024). Adversarial-learning-based Taguchi convolutional fuzzy neural classifier for images of lung cancer. *IEEE Access*, *12*, 72766-72776.

[2] Bidzińska, J.; Szurowska, E. "See Lung Cancer with an AI." *Cancers* **2023**, *15*,1321 https://doi.org/10.3390/cancers15041321.

[3] Bianconi, F., Palumbo, I., Spanu, A., Nuvoli, S., Fravolini, M. L., & Palumbo, B. (2020). "PET/CT Radiomics in Lung Cancer: An Overview." *Applied Sciences*, *10*(5),1718. https://doi.org/10.3390/app10051718.

[4] Pan Feng, Feng Li, Liu Baocai, Hu Yue, Wang Qian. "Application of radiomics in diagnosis and treatment of lung cancer." Front. Pharmacol., 01 November 2023, Sec. Respiratory pharmacology, 14 – 2023, doi.org/10.3389/fphar.2023.1295511

[5] F. Binczyk, Wojciech Prazuch, P. Bożek and J. Polańska. "Radiomics and artificial intelligence in lung cancer screening." *Translational Lung Cancer Research*,10(2021):1186-1199.https://doi.org/10.21037/tlcr-20-708.

[6] Pasini, G., Stefano, A., Russo, G., Comelli, A., Marinozzi, F., & Bini, F. (2023). "Phenotyping the Histopathological Subtypes of Non-Small-Cell Lung Carcinoma: How Beneficial Is Radiomics?" Diagnostics,13(6),1167. https://doi.org/10.3390/diagnostics13061167.

[7] Lin, M., Li, L., Hui, Y. *et al.* "Machine learning-based prediction of invasiveness in lung adenocarcinoma presenting as ground-glass nodules using radiomics and

clinical CT features." *BMC Cancer* **25**, 1693 (2025). https://doi.org/10.1186/s12885-025-14983-3.

[8] Chaunzwa, T.L., Hosny, A., Xu, Y. *et al.* "Deep learning classification of lung cancer histology using CTimages." *SciRep* **11**,5471(2021). https://doi.org/10.1038/s41598-021-84630-x.

[9] Gandhi Z, Gurram P, Amgai B, Lekkala SP, Lokhandwala A, Manne S, Mohammed A, Koshiya H, Dewaswala N, Desai R, et al. "Artificial Intelligence and Lung Cancer: Impact on Improving Patient Outcomes." *Cancers*. 2023; 15(21):5236. https://doi.org/10.3390/cancers15215236.

[10] Cellina M, Cacioppa LM, Cè M, Chiarpenello V, Costa M, Vincenzo Z, Pais D, Bausano MV, Rossini N, Bruno A, et al. "Artificial Intelligence in Lung Cancer Screening: The Future Is Now." *Cancers*. 2023; 15(17):4344. https://doi.org/10.3390/cancers15174344.

[11] Niyaz Ahmad Wani, Ravinder Kumar, Jatin Bedi, "DeepXplainer: An interpretable deep learning based approach for lung cancer detection using explainable artificial intelligence," Computer Methods and Programs in Biomedicine, Volume 243, 2024, 107879, ISSN0169-2607, https://doi.org/10.1016/j.cmpb.2023.107879.

[12] Nishan Rai and Sujan Khatri and Devendra Risal, "Explainable AI Technique in Lung Cancer Detection Using Convolutional Neural Networks," arXiv, 2026, https://arxiv.org/abs/2508.10196.

[13] Alqhatani Abdulmajeed, Babu T. K. S. Rathish, Mahesh T. R., Khan Surbhi Bhatia, Saidani Oumaima , Quasim Mohammad Tabrez, "Automated classification and explainable AI analysis of lung cancer stages using EfficientNet and gradient-weighted class activation mapping," Frontiers in Medicine, Volume 12–2025, doi: 10.3389/fmed.2025.1625183.

[14] Adnan, K.M., Ghazal, T.M., Saleem, M. *et al.* Secure and interpretable lung cancer prediction model using mapreduce private blockchain federated learning and XAI.*SciRep***15**,35693(2025). https://doi.org/10.1038/s41598-025-19478-6

[15] Saied, M., Raafat, M., Yehia, S., & Khalil, M. (2023). "Efficient pulmonary nodules classification using radiomics and different artificial intelligence strategies." *InsightsintoImaging*, https://doi.org/10.1186/s13244-023-01441-6.

[16] S. Malarvannan and M. Angulakshmi, "A Review on Lung Cancer Classification Using Deep Learning Techniques," in *IEEE Access*, vol. 13, pp. 76161-76184, 2025, doi: 10.1109/ACCESS.2025.3564633.

[17] F. Haque *et al.*, "An End-to-End Concatenated CNN Attention Model for the Classification of Lung Cancer with XAI Techniques," in *IEEE Access*, vol. 13, pp. 96317-96336,2025,doi: 10.1109/ACCESS.2025.3572423.

[18] Marjolein A. Heuvelmans, Peter M.A. van Ooijen, Sarim Ather, et al. "Lung cancer prediction by Deep Learning to identify benign lung nodules," Lung Cancer, Volume 54, 2021, Pages 1-4, ISSN 0169-5002, https://doi.org/10.1016/j.lungcan.2021.01.027.

[19] Jiaying Liu, Anna Corti, Valentina D.A. Corino, Luca Mainardi, "Lung nodule classification using radiomics model trained on degraded SDCT images," Computer Methods and Programs in Biomedicine, Volume 257, 2024, 108474, ISSN 0169-2607.doi.org/10.1016/j.cmpb.2024.108474.

[20] P. Aonpong, Y. Iwamoto, X. -H. Han, L. Lin and Y. -W. Chen, "Genotype-Guided Radiomics Signatures for Recurrence Prediction of Non-Small Cell Lung Cancer," in *IEEE Access*, vol. 9, pp. 90244-90254, 2021, doi: 10.1109/ACCESS.2021.3088234.

[21] Lin J, Yu Y, Zhang X, Wang Z, Li S. "Classification of Histological Types and Stages in Non-small Cell Lung Cancer Using Radiomic Features Based on CT Images." J Digit Imaging. 2023 Jun;36(3):1029-1037. doi: 10.1007/s10278-023-00792-2. Epub 2023 Feb 24. PMID: 36828962; PMCID: PMC10287608.

[22] Zahra Khodabakhshi, Shayan Mostafaei, Hossein Arabi, Mehrdad Oveisi, Isaac Shiri, Habib Zaidi, "Non-small cell lung carcinoma histopathological subtype phenotyping using high-dimensional multinomial multiclass CT radiomics signature," Computers in Biology and Medicine, Volume 136, 2021, 104752, ISSN-0010-4825, https://doi.org/10.1016/j.compbiomed.2021.104752.

[23] Hung, S., Wang, Y., & Tseng, M. (2023). "An Interpretable Three-Dimensional Artificial Intelligence Model for Computer-Aided Diagnosis of Lung Nodules in Computed Tomography Images." *Cancers*, 15. https://doi.org/10.3390/cancers15184655.

[24] Hossain, M., Basak, N., Mollah, M., Nahiduzzaman, M., Ahsan, M., & Haider, J. (2025). "Ensemble-based multiclass lung cancer classification using hybrid CNN-

SVD feature extraction and selection method." *PLOS One*, 20. https://doi.org/10.1371/journal.pone.0318219.

[25] C. Y. Kesiku and B. Garcia-Zapirain, "AI-Enhanced Lung Cancer Prediction: A Hybrid Model's Precision Triumph," in *IEEE Journal of Biomedical and Health Informatics*, vol. 29, no. 9, pp. 6287-6300, Sept. 2025, doi: 10.1109/JBHI.2024.3447583.

[26] Shimada, Y., Kudo, Y., Maehara, S. *et al.* "Artificial intelligence-based radiomics for the prediction of nodal metastasis in early-stage lung cancer." *Sci Rep* **13**, 1028 (2023). https://doi.org/10.1038/s41598-023-28242-7.

[27] Hunter, B., Argyros, C., Inglese, M. *et al.* "Radiomics-based decision support tool assists radiologists in small lung nodule classification and improves lung cancer early diagnosis." *Br J Cancer* **129**, 1949–1955 (2023). doi: 10.1038/s41416-023-02480-y. PMID: 37932513; PMCID: PMC10703918.

[28] B. Hunter et al. "A radiomics-based decision support tool improves lung cancer diagnosis in combination with the Herder score in large lung nodules." *eBioMedicine*, 86 (2022). https://doi.org/10.1016/j.ebiom.2022.104344.

[29] Hammad, M., ElAffendi, M., El-Latif, A., Ateya, A., Ali, G., & Pławiak, P. (2025). "Explainable AI for lung cancer detection via a custom CNN on CT images." *Scientific Reports*, 15. https://doi.org/10.1038/s41598-025-97645-5.

[30] Chen, P., Gong, H., Zhang, L., & Geng, Y. (2025). "CT radiomics combined with neural networks predict the malignant degree of pulmonary grinding glass nodules." *Frontiers in Medicine*, 12. https://doi.org/10.3389/fmed.2025.1603472

[31] X. Ma *et al.*, "Survival Prediction for Non-Small Cell Lung Cancer Based on Multimodal Fusion and Deep Learning," in *IEEE Access*, vol. 12, pp. 123236-123249, 2024, doi: 10.1109/ACCESS.2024.3453930.